Review

The influence of combustion properties on the hazards potential of hazard division (HD) 1.3 materials

Cynthia P. Romo*, Kevin P. Ford*, Aubrey D. Farmer*, Alice I. Atwood*†, Thomas L. Boggs*, and Josephine Covino**

*Naval Air Warfare Center Weapons Division, 1 Administration Circle, China Lake, California 93555-6100, UNITED STATES
Phone: +1-760-939-0203
†Corresponding author: alice.atwood.ctr@navy.mil

**DoD Explosives Safety Board, 4800 Mark Center Drive, Suite 16E12, Alexandria, Virginia 22350-3606, UNITED STATES

Received: November 2, 2017 Accepted: February 14, 2018

Abstract

This paper examines the ignition and combustion properties of HD1.3 substances and their influence on the thermally driven hazard threat. Materials that are easier to ignite and burn readily at low pressure are most vulnerable to the thermal threat. The surface area of the energetic material plays a strong role in the pressurization rate and subsequent reaction response of the energetic material. A series of subscale combustions tests in a concrete structure are being used to further examine the hazard response of an HD1.3 substance, to a combustion driven stimulus.

Keywords: combustion driven hazards, burning rate, hazard divisions 1.1 and 1.3, deflagration, detonation

1. Introduction

1.1 This report is part of an ongoing effort by the United States Department of Defense Explosive Safety Board (DDESB) to review the methods for determining the safe separation distances of items and bulk materials that represent a mass to moderate fire hazard (classified as Hazard Division (HD) 1.3 and HD1.4). The work is not complete, and this paper is presented not only to examine the hazard potential of combustion driven events but also to identify areas where further data are needed.

1.2 Combustion driven hazard threats exist throughout the entire life cycle of an energetic material or item; spanning from synthesis, manufacture, transportation and storage, performance, and disposal. A most simplistic view of the threat is given in Figure 1. The energy content and physical state of the sample play a major role in its response to a specific stimulus. Likewise, the environment surrounding the item at the stimulus application will be a controlling factor. The type, amplitude, and duration of the stimulus must also be considered. An example of varying responses would be the high surface area of a granular gun propellant versus that of a large solid rocket propellant stored in an earth covered magazine or reinforced concrete with high confinement compared to that of an ISO container. Combustion driven events are relatively long duration when compared to a shock driven event. This difference can lead to very different responses.

1.3 Boggs et al.[1] provides a review of accidents from the beginning of the 20th century to March 2012. This review was made in order to gain an understanding of the predominant stimuli encountered by the energetic sample throughout its life cycle. Fire was identified as the primary event in 75 percent of the 141 incidents reviewed in this study. Most of the accidents had fire as the primary stimulus, not explosions or detonations. Often the fires burned for a significant time before either burning out or transitioning to an explosion or detonation.

1.4 The focus of this paper will be on the response of the energetic to a thermal stimulus due to its frequency of occurrence in a storage and transportation environment. A thermal stimulus may occur internally, due to decomposition and self-heating of the energetic from stabilizer depletion or ingredient incompatibility. The stimulus may also be applied externally, in the case of an

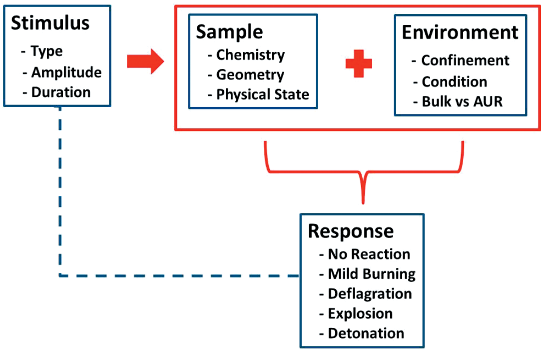

Figure 1 A simplified view of the combustion driven hazard threat.

adjacent fire (often referred to as cookoff), electrical malfunction, or transportation fire (hot brakes, collision).

1.5 The response of an item can vary from no reaction to burning, deflagration, explosion and detonation. There is a desire to reduce the probability of a detonation, but the reactions of burning to explosion may be, in some cases, more problematic and will likely increase in frequency with the incorporation of insensitive munitions into the fleet[2).

1.6 Characterization of the energetic fill is most often performed to gain an understanding of its required performance; however, an understanding of the contribution of a specific performance behavior to a potential hazard response cannot be ignored.

2. Background

2.1 Nine hazard classes make up the hazard classification system and are listed in Table 1. Explosives, propellants, and pyrotechnics are included in Hazard Class 1. The Class 1 hazard has been assigned six hazard divisions to further describe the character of the explosive hazard. The six Class 1 hazard divisions are listed in Table 2. HD 1.2.x has been further divided to describe the characteristics of the fragments an energetic item might produce[3).

2.2 Hazard classification addresses hazard threats and conditions for transportation and storage configurations only and does not consider operational hazard threats and conditions such as those listed in Table 3.

2.3 HD1.3 includes substances and articles that present a mass fire hazard with a minor blast and/or fragment hazard. HD1.4 includes substances and articles that present a moderate fire hazard with no blast or fragment hazard. The hazard for HD1.1 substances and articles, in contrast, is mass detonation/explosion, producing blast overpressures as the primary effect. Thermal hazards are the dominant HD1.3 response, and the mass conversion rates and heat fluxes are of particular importance when considering the output of these items. HD1.3 covers a broad range of ordnance from small grenades and gun propellants to large diameter solid rocket motors and will be the focus of this paper. An assessment of the U.S. Navy inventory provided a means to identify the most common and the most reactive items, and therefore the most likely to be involved in an incident, that make up the hazard divisions of 1.1, 1.3, and 1.4[4).

Table 1 Nine ammunition and explosives hazards classes (Reference 3).

Hazard class	Material
Class 1	Explosives
Class 2	Gases
Class 3	Flammable liquids
Class 4	Flammable solids
Class 5	Oxidizing substances and organic peroxides
Class 6	Toxic and infectious substances
Class 7	Radioactive materials
Class 8	Corrosive substances
Class 9	Miscellaneous dangerous substances and articles

Table 2 Hazard class 1 divisions (Reference 3).

Hazard division	Hazard type
1.1	Mass explosion
1.2.x	Non-mass explosion, fragment producing
1.3	Mass fire, minor blast or fragment
1.4	Moderate fire, no significant blast or fragment
1.5	Explosive substance, very insensitive (with mass explosion hazard)
1.6	Explosive article, extremely insensitive (no mass explosion hazard)

Table 3 Hazards not considered in classification (Reference 23).

Hazard exclusions
Electrostatic and electromagnetic influence
Rough handling and vibration
Effects of exposure to hot or cold environments
Mechanical defects
Solar radiation
Temperature shock
Abnormal functioning
Combat exposure
Ionizing radiation

2.4 Propellants and explosives are energetic materials found in missile motors, bombs, and warheads, as well as in bulk powder and as the fill in gun cartridges and projectiles. The materials can burn, explode, and/or detonate either on purpose or by accident. These accidents can occur during manufacture, transportation, storage, and operational use. One way to protect personnel and facilities from the risk and consequences of accidents caused by inadvertent reaction of these energetic materials is to provide safe-separation distances between possible explosive sources and exposed sites whether they are inhabited buildings, public roadways, or processing buildings.

2.5 The methods for determining safe-separation distances for the U.S. Department of Defense are contained in DOD Ammunition and Explosive Safety Standards, DOD 6055.09-M[5). This document presents various HD classifications and the methods for determining the safe-separation distances for each HD and /or mixed storage involving multiple HD classifications.

2.6 The methods (predominantly tables and equations) presented in DOD 6055.09-M are largely based on the relationship

$$D = kW^{1/3} \quad (1)$$

where:

D = distance in feet

k = a factor that depends on HD and other considerations

W = net explosive weight of energetic material in pounds

2.7 D is often referred to as the Quantity-Distance (Q-D) for the given weight (quantity) of energetic material. Safe-separation distances, or quantity-distance (Q-D), are currently determined for the various HDs, with emphasis on HD1.1. Most of the methods used to evaluate Q-D for a given energetic material are based on the assumption that the worst case reaction is detonation-like. Subscale combustion experiments with HD1.3 gun propellant in concrete structures have been performed to examine the accuracy of the safe-separation distances calculated by this approach for an HD1.3 substance[6),7)].

2.8 Earlier experimental studies[8),9)] showed that even when a mass fire did not transition to an explosion or detonation, if confined in a robust structure such as an earth-covered magazine with insufficient venting, pressure inside the structure could rapidly build and cause rupture of the structure. The pressure induced rupture can throw large pieces of structural debris long distances without evidence of a blast over-pressure or cratering. These experimental studies also showed that even when the structure does not catastrophically rupture, plumes from mass fires can extend several hundred feet from the structure. Any personnel in the path of the plume are likely to perish, and personnel can also perish if exposed to radiation from the plume given sufficient heat flux-exposure time to cause second- and third-degree burns.

3. Sample selection

3.1 Each of the hazard divisions was searched by both number and weight to gain an understanding of what items present the greatest risk in the Navy inventory. The inventory was examined in two ways in order to identify the items most likely to be found in a magazine (largest numbers) and to identify the items that contain the largest amount of energetic material (present largest potential reactivity)[4)].

3.2 The Navy conventional ordnance stockpile consists of items ranging from small arms ammunition to cruise missiles. The ordnance inventory was examined by both number of occurring Navy Stock Numbers (NSNs), such as with the small ammunition, and by Net Explosive Weight (NEW), which includes guided missiles. The four hazard class/divisions sorted by NSN numbers are summarized in Figure 2. The sort by number gives an indication of the kind and type of items that are most likely to be found in a storage magazine. HD1.4 ordnance

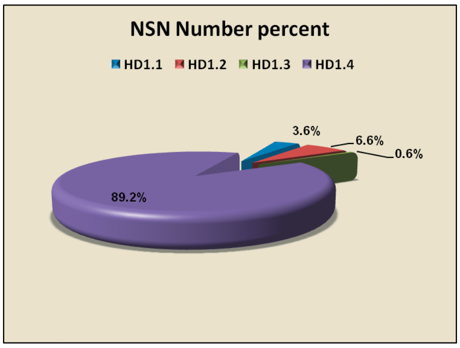

Figure 2 Summary of the Navy ordnance inventory by number of occurring NSNs.

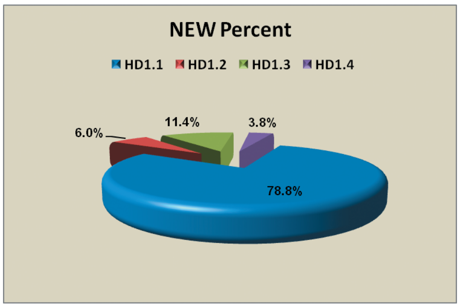

Figure 3 Summary of the Navy ordnance inventory by NEW.

makes up the majority (by number), approximately 89 percent, of the four groups. HD1.3 makes up approximately 0.6 percent by number. Combined, the HD 1.3 and HD1.4 make up about 90 percent of the items most likely to be found in a storage magazine.

3.3 The four hazard class/divisions sorted by NEW are summarized in Figure 3. The sort by NEW gives an indication of those items containing the largest amount of energetic material. Ordnance of HD1.1 makes up the majority (by NEW), approximately 79 percent, of the four groups with the HD1.3 making up approximately 11 percent by weight.

3.4 It should be pointed out that the HD1.3 group is often found in mixed storage with HD1.1 items and, thus, stored at the higher classification level. The HD1.3 group is further complicated by its broad diversity, ranging from high surface area bulk gun propellant to large rocket motors. Various HD1.1 and 1.3 substances have been selected to describe the critical characteristics of these materials relative to the thermal threat. A bulk, HD1.3, nitrocellulose-based gun propellant sample was selected for the subscale testing described in this report based on the above studies.

4. Combustion characteristics

4.1 Ignition

4.1.1 Ignition of an energetic material can occur as the result of an applied stimulus or auto-ignition/self-heating. The auto-ignition temperature is defined as the bulk temperature at which irreversible exothermicity will progress without the addition of an external thermal stimulus. This paper will focus on the response of an energetic material to an external thermal flux; however, the importance of auto-ignition relative to the hazards response of an energetic should be noted.

4.1.2 A contributing factor to the susceptibility of a solid energetic material, such as that found in a rocket motor, to inadvertent ignition has been attributed to what Caveny refers to as propellant flammability[10]. This includes (a) propellant ignitability, which in this case is the exothermic propellant response with application of an external heat source; (b) flame retention, or the ability of the propellant to self-sustain upon removal of the external heat flux; and (c) flame spreading, or the ability for propellant adjacent to the ignition site to become ignited[11]. The data reported in this paper seek to address the combination of what the above authors refer to as ignitability and flame retention, recognizing that flame spread is geometry dependent and not a characteristic of a given energetic formulation. The sample geometry effects, with respect to surface area and combustion, will be addressed in a later section.

4.1.3 Ignitability of a solid energetic, in this context, is considered as not just a process, but the successful completion of the process resulting in steady-state combustion[12]. Ignitability is illustrated in the general log-time versus log-energy flux plot of Figure 4. If a thermal flux level is selected, as indicated by the dashed blue line, first there is a period of inert heating as time progresses. If the external flux is removed at that point, there is no apparent change in the sample, but there is heating of the sample and the formation of a thermal profile at the surface of the propellant. Mildly exothermic reactions will begin to occur as time increases (indicated by the first black line in the figure), and the sample will begin to gasify and light will be generated (measured by a photo diode in the experiment). If the external energy flux is removed at this point, the sample will not continue to burn. It is not until thermal exposure exceeds the second solid line, referred to as the go/no-go ignition locus, that the material will continue to burn if the external flux is removed. The thermal profile has been established, and the flame is sufficiently stable and close enough to the surface to sustain reaction without the external stimulus. The relationship between the two lines is dependent on many variables, including pressure, flux level, and formulation type.[13]

4.1.4 Photographs (Figure 5) of HD1.3 propellant samples (located in the center of each image) that have been exposed at 837 W/cm^2 (200 cal/cm^2-sec) for various amounts of time illustrate the regions of the ignition plot. Figure 5(a) has been exposed for a time less than that defined by the first light/gasification line. No visible changes to the sample surface can be detected. Figure 5(b) has been exposed for time representing the first light/gasification line, and Figure 5(c) has been exposed for time slightly less than that defined by the go/no-go point. Definitions than will be used in this paper include first light or first gasification and go/no-go or complete ignition, which is closer to the point of flame retention referred to previously. The time between first light and go/no-go is referred to as ignition delay.

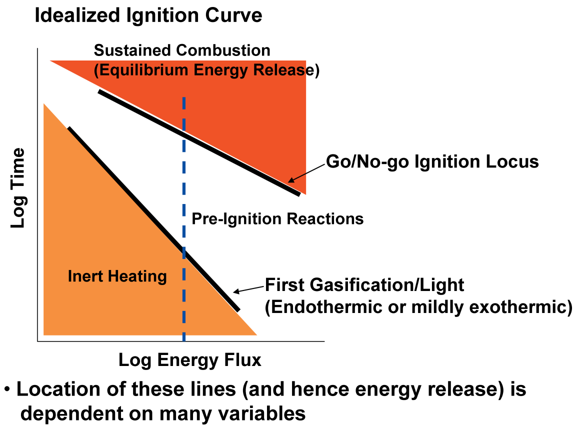

Figure 4 Idealized log-flux versus log-time plot illustrating propellant ignitability.

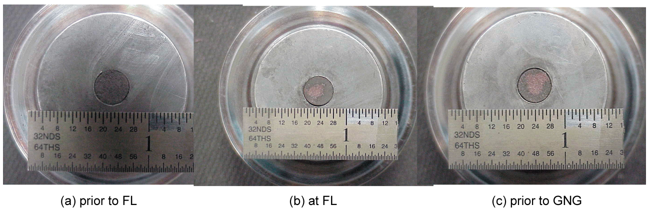

Figure 5 Example of propellant after exposure of thermal flux exposure.

4.1.5 Ignition experiment

4.1.5.1 The ignition data presented in this report were generated with a CO_2 laser ignition system. The energy source was a Photon Sources Model 300 CO_2 laser. The laser was average rated at 450 watts at a wavelength of 10.6 μm. The average variation in thermal flux calibration was about 4 percent, but might range as high as 6 percent at some energy levels. The useable energy range for this experiment was from 12 to 12,553 W/cm^2 (1 to 3000 cal/cm^2-sec).

4.1.5.2 A minimum of 17 samples were used to determine the propellant ignitability at a given flux level. The first gasification line was the average of the photodiode measurements. Complete ignition (GNG), the second line, is determined by means of a Bruceton method of testing and represents the 50% probability point for ignition.

4.1.5.3 The ignitability of HD1.1 and 1.3 solid materials will be examined in this report from a hazards perspective. The effects of pressure and thermal flux on FL and GNG times for various solid energetic will be presented. Further formulation effects on propellant ignitability can be found in Atwood[14].

4.1.6 Radiant ignition data

4.1.6.1 The effect of increasing incident flux on propellant ignitability is illustrated with an HD1.3, Ammonium Perchlorate-based propellant in Figure 6 at 0.09 MPa (1 atm). At relatively low energy levels, the time to first gasification and complete ignition is essentially the same. As the flux increases, the time between FL and GNG increases. The distinction between the two regimes is more definite at higher thermal flux levels.

4.1.6.2 The effect of pressure on propellant ignitability is illustrated for an HD1.3, non-catalyzed AP/HTPB/Al

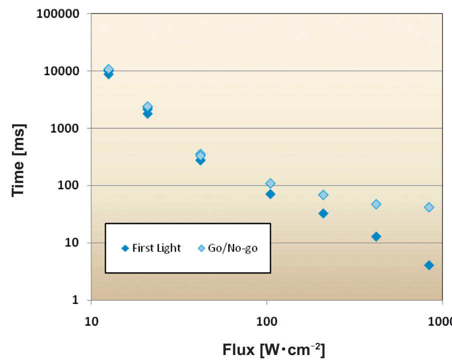

Figure 6 Effect of incident flux levels on HD1.3 propellant ignitability.

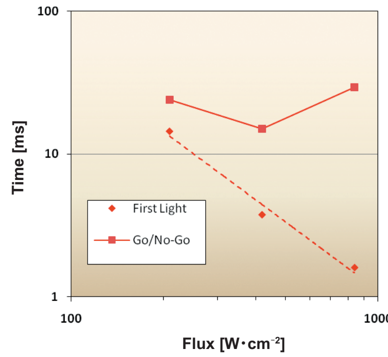

Figure 8 Ignition behavior of M10 gun propellant (250 psia), 1.72 MPa.

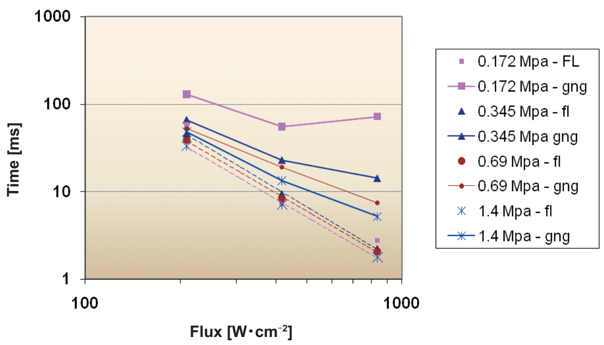

Figure 7 Pressure and flux effects on propellant ignitability.

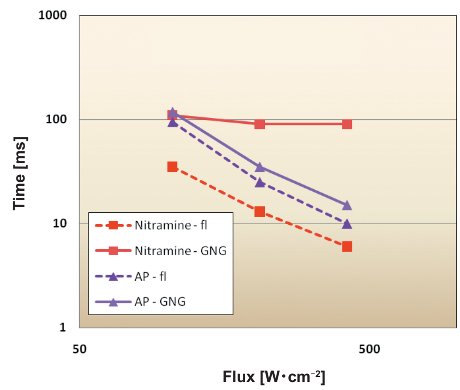

Figure 9 A comparison of HD1.1 and 1.3 substance ignition (0.69 MPa).

propellant in Figure 7. The sample was tested at pressures from 0.17 to 1.38 MPa (25 to 200 psia). The effect of pressure on the first gasification of the propellant is relatively small, while the effect on complete ignition is large, particularly at the higher flux levels. The times between FL and GNG decrease as the pressure increases. The average slope of the FL lines was −2.1. The long times to complete ignition observed at 0.17 MPa (25 psia) indicate overdriven ignition at the higher flux levels[15].

4.1.6.3 The overdriven ignition condition is again illustrated in Figure 8, for the nitrocellulose based, HD1.3 gun propellant, M10[16]. The overdriven condition occurs most often at lower pressures and higher incident flux conditions and has been more commonly observed in single- and double-base formulations. It is important to note the factor of 10 in pressure between the AP and the nitro-based formulations where the phenomenon occurs– at 0.172 MPa (25 psia) in the case of the AP-based propellant, and at 1.72 MPa (250 psia) in the nitrocellulose formulation. The overdriven condition is created when the thermal flux is removed prior to the establishment of an adequate thermal profile at the surface of the energetic material. The formation of highly reactive gaseous products in the absence of complete ignition may also be a contributing factor to reaction violence in an unplanned thermal event.

4.1.6.4 A comparison of the ignitability for a small critical diameter HD1.1 substance and a large critical diameter HD1.3 substance can be seen in Figure 9 for a nitramine-based HD1.1 propellant and a HD1.3 AP-based propellant. The two substances were tested at 0.69 MPa pressure. The nitramine containing propellant is also nitro-plasticized and is readily gasified. In contrast, the AP-based propellant gasifies after a longer exposure and is immediately followed by complete combustion. Complete ignition is not achieved in the nitramine-based propellant until an exposure time of nearly 100 msec is applied. The lengthy pre-ignition period, which is characteristic of formulations of this type, allows for the accumulation of highly reactive pre-ignition products that can play a significant role in the deflagration-to-detonation (DDT) hazard[17], while the easily ignited HD1.3 material presents the greater thermal hazard.

4.1.6.5 The ease of ignition in AP-based materials presents another hazard concern relative to handling, processing, and storage. These typically HD1.3 substances will ignite and burn at low pressure and represent a thermal rather than a blast threat. Ballistic modification can be achieved in the AP composite propellants by changing the particle size of the oxidizer. The burning rate of the propellant can be increased by increasing the amount of "fine" fraction AP added to the formulation. The effect of AP particle size on ignitability is illustrated in the plot of Figure 10. Generally, within a family of propellants, the higher the burning rate the easier the propellant is to ignite, thus increasing its hazard potential with respect to the thermal threat. The burning rates for the propellants in Figure 10 will be presented in the following section.

4.1.7 Burning rate

4.1.7.1 The propellant burning rate pressure and temperature sensitivity are fundamental ballistic properties of a specific formulation. The ingredients of the

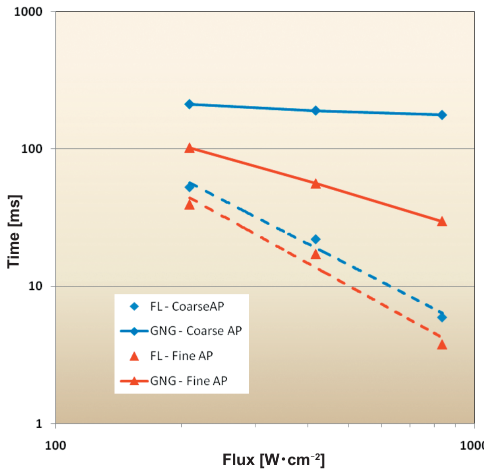

Figure 10 AP particles size effect on ignitability (HD1.3, 0.69 MPa).

formulations are tailored to meet specific performance requirements with respect to burning rate. Understanding the propellant burning rate is vital not only to propellant performance but also in its hazards response. The burning rate behavior of explosives and other HD1.1 substances is also of interest in the evaluation of combustion driven hazards such as cookoff[18].

4.1.7.2 The burning rate of an energetic material is often described over a specific pressure range using the empirical relationship in Equation (2).

$$r_b = c \cdot p^n \tag{2}$$

4.1.7.3 According to a commonly accepted but approximate view, c is an empirical constant influenced by the ambient temperature, and the exponent n is known as the burning rate pressure exponent[19]. The burning rate pressure exponent is independent of the temperature but describes the influence of pressure on the burning rate. Typically, propellants are formulated with a burning rate pressure exponent less than unity. As n approaches unity, the burning rate becomes very sensitive to small changes in pressure, and the effects on performance can be catastrophic.

4.1.7.4 The dependence of burning rate on initial temperature is of particular importance for systems that must operate over a wide range of temperatures. The temperature dependence of the burning rate should be as low as possible in this case. Temperature effects on burning rates are also important to hazards because the ordnance system is often at an elevated temperature when it ignites during these events. Temperature sensitivity of burning rate alone cannot account for the levels of violence often observed in the combustion/thermal hazard referred to as cookoff.

4.1.7.5 High pressure burning rates, such as those of gun propellants, are indirectly determined from the recorded pressure-time history of a manometric or closed bomb using the appropriate thermochemical data and geometric form function describing the sample. The pressure-time data may also be differentiated with respect to time and the resulting dp/dt or quickness data determined. The closed bomb reduction program (CBRED)[20] was used to transform the measured pressurization data into gasified mass regression data.

4.1.7.6 The mass gasification rate is defined in Equation (3):

$$\dot{m}_p = \rho_s \cdot A_b \cdot r \tag{3}$$

where

$\dot{m}_p$ = Mass rate of gasification

ρ_s = Solid density of the material
A_b = Burning area f (time, distance burned)
r = Linear burning rate

4.1.7.7 The burning area is introduced through a geometrical form function and the characteristic dimensions. This allows for a calculation of the linear burning rate as a function of time and, by cross-reference, pressure.

4.1.8 Burning rate experiment

4.1.8.1 Two separate experiments were used to generate burning rate data at pressures from 0.69 MPa (100 psia) to 278 MPa (40 Kpsia). Data from pressures of 0.69 to 10.34 MPa were generated using cinephotomicrography[21], while the remaining data were generated using a closed bomb combustion technique[22].

4.1.9 Burning rate data

4.1.9.1 The burning rates versus pressure are plotted in Figure 11 for the two HD1.3 AP-based propellants of Figure 10. It can be seen that the propellant with the fine AP, which was easiest to ignite, also has the higher burning rate. It can also be seen that care must be taken in the application of Equation (2) as the log burning rate versus log pressure plot is not always linear and tends to form an “s” curve if a wide enough pressure range is included. Burning rate measurements for performance purposes do not usually include such a broad pressure range; however, the behavior of an energetic material in a hazard event can often be linked to its burning rate at the extreme pressures.

4.1.9.2 Energetic materials that will ignite and burn at low pressures present a particular handling concern, and the HD1.3 AP-based composite solid propellants, for example, often demonstrate this characteristic. HD1.1 substances, in contrast, generally burn very poorly at low pressure. At the high pressures, the burning rate pressure exponent can be at or close to unity, a condition that may contribute to increased reaction violence in high confinement hazard conditions.

4.1.9.3 The burning rate of an HD1.3 AP-based propellant is compared to a nitramine-based HD1.1 explosive in Figure 12. The burning rate pressure exponent of the HD 1.1 explosive is at or greater than unity over most of the pressure range in this plot.

4.1.9.4 The effect of initial temperature on burning rate is illustrated with the HD1.3 nitrocellulose-based propellant, M10, in Figure 13. In many cases, the burning rate

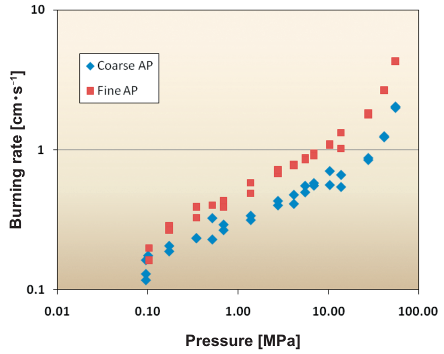

Figure 11 Burning rate versus pressure for two HD1.3 AP-based propellants.

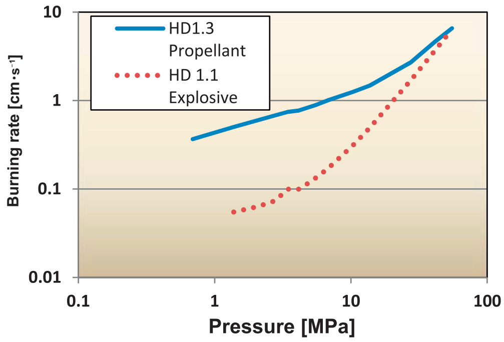

Figure 12 A burning rate comparison.

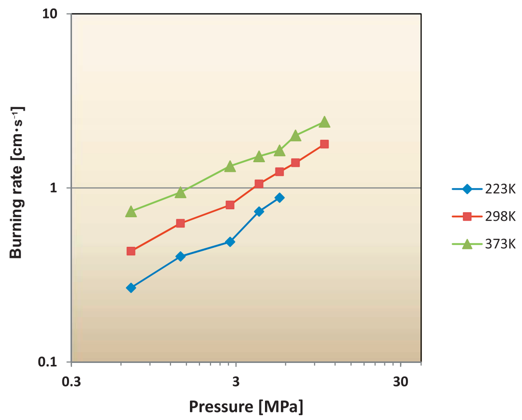

Figure 13 M10 burning rates at three initial temperatures.

temperature sensitivity is highest at low pressure, as is the case with M10 where the sensitivity to burning rate is about 0.9 percent per degree K between ambient and 373 K at 0.69 MPa and about 0.5 percent per degree K at 10.34 MPa.

4.1.9.5 Understanding the effect of initial temperature on the burning rate is critical to propellant performance, and the effect of temperatures on burning rate at or near the cookoff temperature is also of interest. It should be noted that a high burning rate propellant sensitivity does not account for the level of violence observed in most slow cookoff scenarios. The physical and chemical changes that occur in the energetic material at temperature are the dominant contributors to slow cookoff reaction violence.

4.1.9.6 The effect of time-at-temperature on burning rates measured using the optical technique is illustrated for an HD1.3 hydroxy-terminated polyethylene (HTPE) propellant in the normalized plot of Figure 14. The

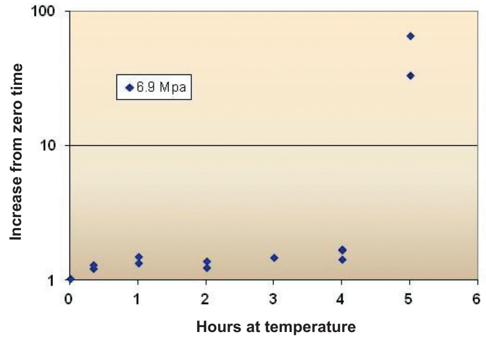

Figure 14 Effect of time at temperature on burning rate.

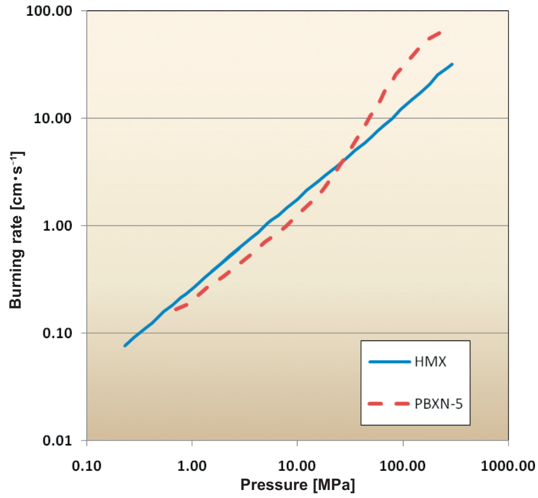

Figure 15 Burning rate versus pressure for PBXN-5 and HMX.

propellant samples were heated at 105°C for up to 5 hours, and their burning rates measured at 6.9 MPa. The small changes in burning rate observed up to 4 hours represent the burning rate sensitivity, and those after 5 hours at temperature illustrate the effect of the physical and chemical changes that have occurred in the material.

4.1.9.7 The burning rate of the HD1.1 explosive PBXN-5 is compared to that of neat cyclotetramethylene tetranitramine (HMX) in Figure 15. The explosive, PBXN-5, is composed of 95 weight percent HMX and 5 percent Viton A as binder. The HMX burning rate curve is a combination of large single crystals, pressed pellets measured with the optical technique, and carefully screened powder measured in with the closed bomb technique[23]. The PBXN-5 was composed of small agglomerates of HMX coated with the binder[24]. The PBXN-5 burning rate curve is a combination of pressed pellets using the optical technique and powder in the closed bomb technique[25].

4.1.9.8 Several features can be identified in Figure 15. The burning rate pressure exponent for neat HMX over the measured pressure range is 0.84; this rate is quite typical of nitramines and their formulations. Up to about 29 MPa, the PBXN-5 burning rate is lower than that of the neat HMX; this rate is also typical of nitramine-based formulations. Above 29 MPa, there is a change in the burning rate pressure exponent with a transition to a higher burning rate. This feature has been attributed to a

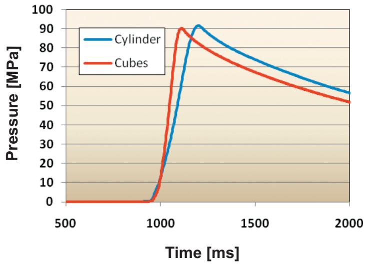

Figure 16 (a) Pressure-time history for an HD1.3 propellant.

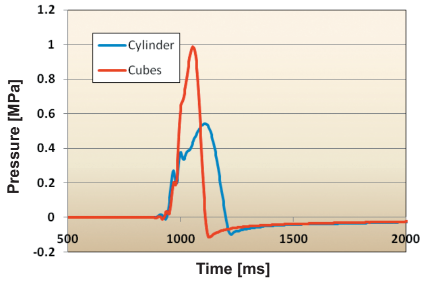

Figure 16 (b) Effect of surface area in differentiation of pressure-time history.

Table 4 M1 propellant loading.

Test #	Grain type	Weight [kg]	Loading density [g·cm^{-3}]	drums
1	1P	135	0.017	3
2	1P	535	0.067	8
3	7P	120	0.015	3
4	7P	503	0.063	8
5	7P	120	0.015	3
6	7P	535	0.063	7
7	7P	240	0.030	3

deconsolidation of the explosive agglomerates and a change from conductive to convective burning[26].

4.1.9.9 Convective burning is characterized by the rapid penetration of hot gases that control the propagation rate through convective heat transfer. It is considered to be a key factor in deflagration to detonation (DDT). The requirements for DDT to occur are a sufficient surface-to-volume ratio and porosity of the energetic sample either through manufacture and loading, as in the case of some gun propellants, or through large-scale damage in the case of missile propellants. Convective combustion and DDT must be considered when deflagration precedes the explosive or detonative incident. The DDT hazard has been studied extensively, and the reader is referred to the extensive bibliography found in AGARDograph No. 316[27] for more details on the subject.

4.1.9.10 Under the appropriate conditions, DDT can occur in substances other than HD1.1, as was the case in the PEPCON incident of 4 May 1988, in Henderson, Nevada, where several thousand tons of AP in the plant were involved in the resulting reactions[28].

4.2 Surface area

4.2.1 Although not an intrinsic property of the energetic material, from Equation (3) above, it can be seen that the

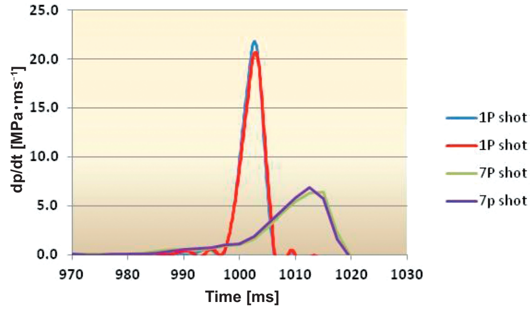

Figure 17 Surface area effects on closed bomb pressurization rate.

surface area plays a key role in the mass reduction rate of the energetic substance. As the burning area, A_b, increases, the mass reduction rate also increases. The effect of surface area on the pressure-time history for a substance is illustrated for an AP-based HD1.3 propellant in Figure 16 (a). The propellant was burned at the same loading density (~0.09 gm/cm^3) in each shot ; however, in one case, it was cut into a single 17 mm diameter cylinder and, in the other, seven 1 cm cubes. The effect changing the surface area on pressurization rate is illustrated in the plot of the pressure differential versus time of Figure 16 (b). The implication on a combustion driven hazards threat is that the geometry of the energetic material, no matter what the hazard classification, will have a strong effect on the response of the item in the absence of sufficient venting.

4.2.2 Either mechanical or thermal insult to an energetic during a hazard incident can substantially increase the burning area of an energetic material. The type and extent of damage induced into an energetic material is an important consideration in the evaluation of a hazards threat. Introduction of only 1 to 4 percent voids can have a significant effect on shock sensitivity[29]. The probability and severity of DDT in damaged energetic material is linked to the type and extent of damage that can be generated in the material.

5. Subscale magazine testing

5.1 Sample

5.1.1 Seven subscale magazine tests were performed with the HD1.3, nitrocellulose (NC) based gun propellant M1. This propellant was selected as it represents a sample similar to those found in large numbers in the Navy inventory. It was also selected in order to compare the results of the current tests with those of previous investigators[8), 9]. Combustion tests in subscale magazines were performed to evaluate the role of gun propellant surface area and loading density relative to venting, pressurization, plume, and fireball formation[5] in a concrete structure. It is recognized that the M1 formulation does not represent the most energetic of HD 1.3 gun propellants. A summary of the loading configuration used in the subscale testing is given in Table 4. Testing was conducted on two different M1 Grain configurations : a single perforation grain (1P) and a seven perforated grain (7P). The testing of the 1P grain was reduced due to limited availability of that geometry. Tests

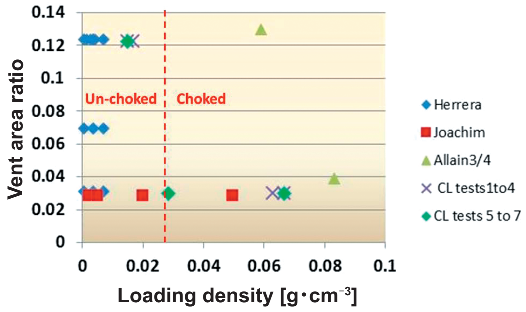

Figure 18 Vent area ratio versus loading density for M1 subscale testing.

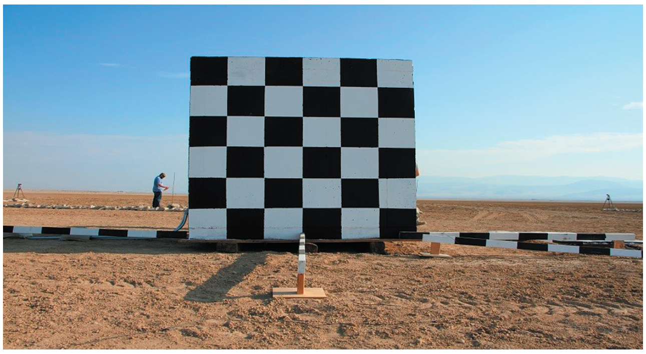

Figure 19 Kasun structure used in HD1.3 M1 propellant testing.

2 and 4 will be the primary focus of this report.

5.1.2 The propellant for each test was contained in fiber drums 49.53 cm (19.5 inches) in diameter and 67.31 cm (26.5 inches) in height, with their lids buckled. The propellant was poured in until it reached a height 38.1 cm (15 inches) below the top of the barrel. Test 2 contained a total of 535 kg (1176 lbs) of propellant. Test 4 had a total of 503 kg (1108 lbs) of propellant. The gun propellant was initiated using point-source igniters, which were placed in each of the drums. The igniters were simultaneously initiated using an electric match firing into a 113.5 g (0.25 lb) bag of smokeless powder acting as aide.

5.1.3 The effect of M1 propellant surface area on closed bomb pressurization rate is illustrated for the smaller, single (1P) and the larger 7 perforation (7P) granules in Figure 17. The 1P, M1 grains have the larger surface area.

5.2 Confinement/structure (environment)

5.2.1 The pressurization of a structure is a competition between the pressure produced from reacting the solid energetic material to product gases and its release by the gases leaving the structure through venting. The pressurization due to reaction from solid energetic material to product gases is dependent on the density of the solid, the surface regression rate of the solid (often called the linear burning rate), the burning surface area, and the thermochemistry of the reaction (Equation (2)). Because gun propellants have high surface area available for combustion, they produce rapid pressurization. Choked flow occurs when the pressure inside a vessel or structure is about twice that of the pressure outside the structure. Once the flow is choked, pressure inside the structure can increase rapidly as the energetic material burns inside the

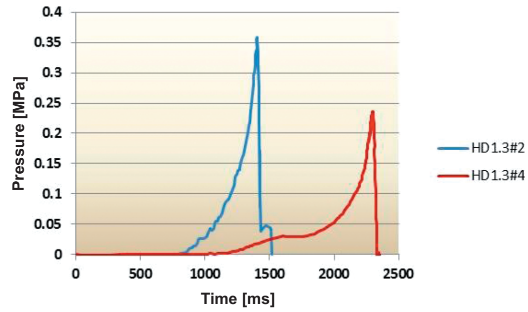

Figure 20 Pressure-time curves for test 2 and test 4.

structure.

5.2.2 The non-dimensional vent area ratio (VAR) is a term used to describe venting (Equation (4)).

$$\mathrm{VAR} = (A_v / V_{ch})^{2/3} \tag{4}$$

where

A_v = area of the vent
V_{ch} = Chamber volume

The *loading density* of energetic material is defined as the weight of energetic material divided by the volume of the structure. A high vent area ratio and a relatively low loading density are needed for a structure to survive pressurization. HD1.3 Tests 2 and 4 had a loading density of 0.06668 and 0.06288 g/cm^3, respectively. Figure 18 presents a plot of the vent area ratio versus the loading density for the tests of Table 4 and several tests described in Allain[8] and Herrera et al.[9] The tests at an M1 loading density greater than 0.03 g/cm^3 resulted in rupture of the structure and, thus, choked flow, while those with less than 0.03 g/cm^3 where the structure survived were unchoked.

5.2.3 The Swedish structure, known as a Kasun[30], shown in Figure 19 was selected as a subscale test vehicle as the 2 m × 2 m × 2 m geometry had been previously used for testing of M1 gun propellant (seen in Figure 18), and it was also used in studies of HD1.1 explosive charges with respect to detonation.

5.2.4 All seven subscale tests were vented. Tests 1, 3, and 5 were assembled with a 79 cm diameter orifice and did not fail (unchoked condition). Tests 2, 4, 6, and 7 were assembled with a 39 cm orifice and all failed (choked condition), including Test 7 with the lower loading density. The construction of the structure was modified for Tests 5 through 7 with increased rebar tying the walls and door to the roof of the structure.

5.2.5 The tests were internally and externally instrumented using pressure, temperature, and heat flux gages. The interior walls of the structure were color coded in order to identify the fragment source. External high-speed digital video, Doppler velocimetry, and infrared camera coverage were also included.

5.2.6 Three hundred and sixty degree fragment mapping was performed for the tests that resulted in structural failure.

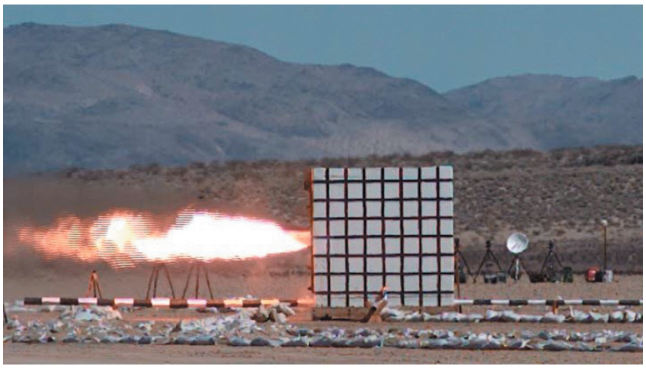

Figure 21 Illustration of plume, still photograph from high-speed video, test 4.

Figure 22 Illustration of fireball, still photo from high-speed video, test 4.

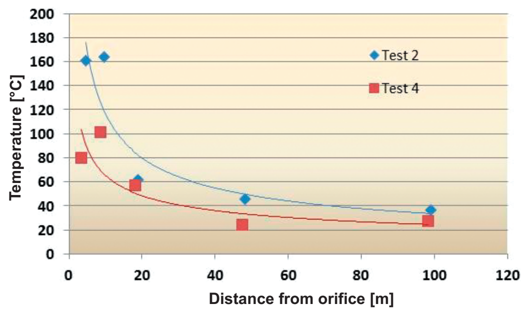

Figure 23 Maximum temperature measured at a distance in alignment with the structure orifice.

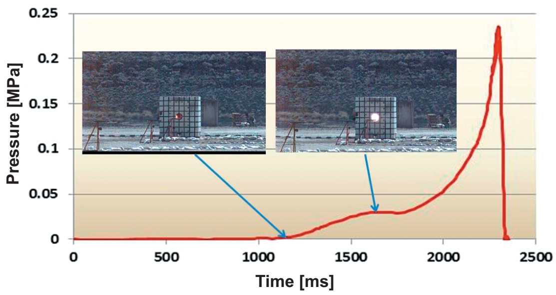

Figure 24 Relating the plume/fireball formation with internal pressure, test 4.

Figure 25 Flamelet exiting in orthogonal view of complete ignition, test 4.

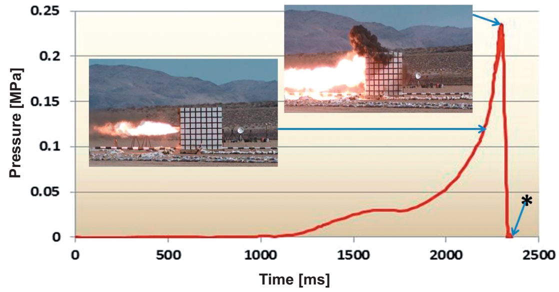

Figure 26 Plume formation and structural failure, test 4.

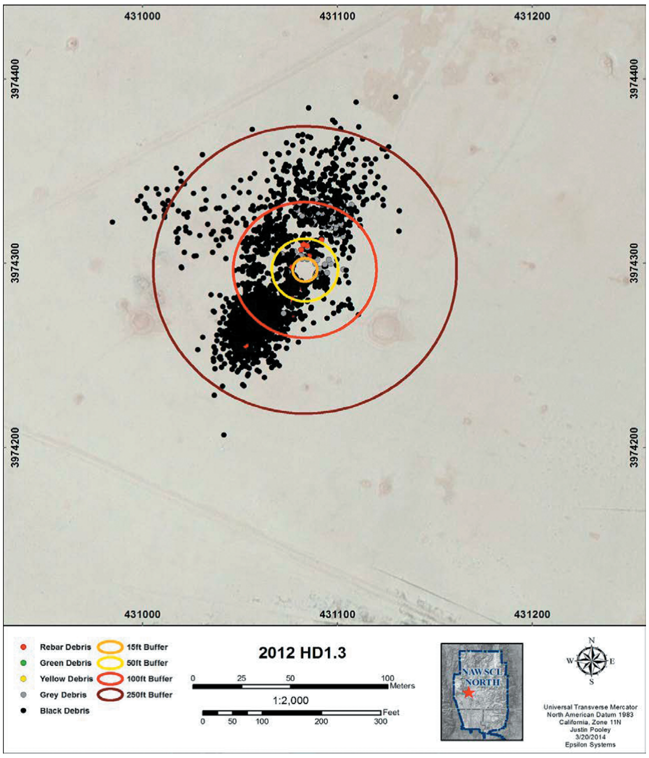

Figure 27 Fragment map of test 2.

5.3 Response

5.3.1 The effect of the M1 propellant surface area on the structure interior pressurization can be seen in Figure 20. The structure from Test 2 ruptured 1.4 seconds after the ignition of the firing train; whereas, the structure from Test 4 ruptured at 2.3 seconds. The rupture pressure measured for Test 2 was 0.234 MPa (34 psi) and 0.324 MPa (47 psi) for Test 4. The difference between Test 2 and Test 4 was due to the geometry of the M1 propellant, which led to differences in propellant mass burning and interior pressurization rates between 1P and 7P pellets. Plume and fireball formation are illustrated in Figures 21 and 22, respectively (Test 4).

5.3.2 A comparison of the maximum temperature measured externally in alignment with the orifice of the structure for Tests 2 and 4 is given in Figure 23. Maximum temperatures were slightly lower for Test 4 than for Test 2; however, the differences may also be related to the prevailing wind conditions as these temperatures were measured externally after structure failure. A maximum thermal flux measured in the fireball

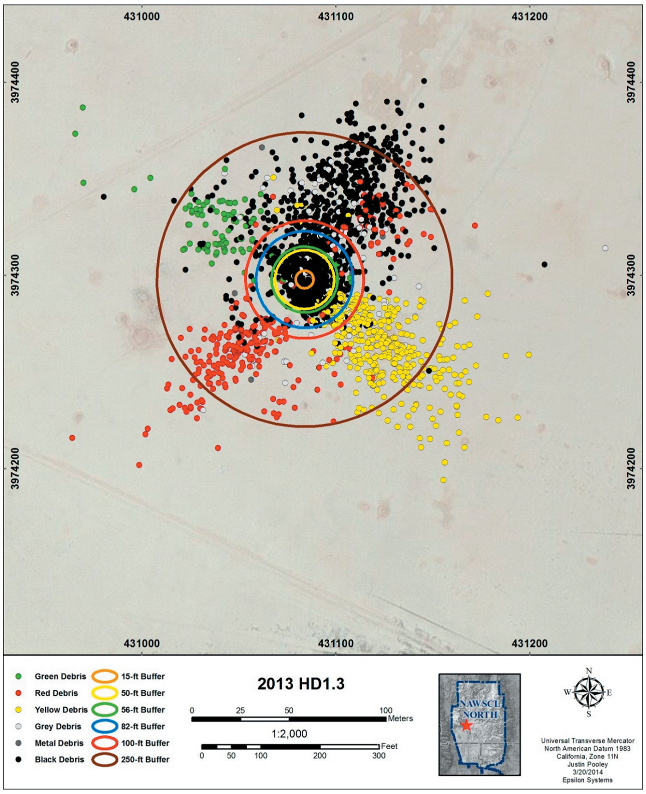

Figure 28 Fragment map of test 4.

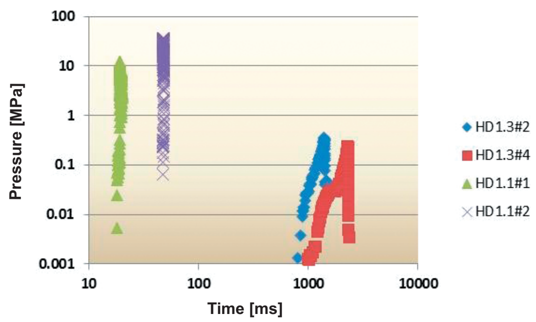

Figure 29 Time difference between the prompt shock and combustion driven events.

after the structure failed was measured at 158.22 kW/m^2 and 210.626 kW/m^2 for Tests 2 and 4, respectively.

5.3.3 The reactions observed in the high-speed video can be related to the pressurization curves and are illustrated for Test 4 in Figures 24 and 26. The initial pressurization is related to the first light/gasification of the M1 propellant as seen by the illuminated orifice in Figure 24, at the initial pressure rise followed by complete ignition (fully illuminated orifice in Figure 24). A small flamelet can be seen exiting the structure at the complete ignition time in the orthogonal view of the structure in Figure 25. The later time events of plume formation and failure of the structure are illustrated in Figure 26. Fireball formation and debris throw occurred at the time indicated by the asterisk in Figure 26 and can be seen in Figure 22. The structure failed at the roofline in both of the tests.

5.3.4 The fragment map of Test 2 is given in Figure 27, where the circles indicate distance from the original structure; orange at 4.6 meters (15 feet), yellow at 15.2 meters (50 feet), red at 30.5 meters (100 feet) and brown at 76.2 meters (250 feet). Over 2,609 debris samples were weighed; their color recorded, and their location mapped. The Test 2 fragment map shows that most of the fragments were from the roof (black concrete). Fragments weighing less than 5 grams were not recorded in any of the HD1.3 tests. Additionally, in Test 2, some of the fragments weighing less than 200 grams were not collected in the southern and western areas of the site within the 21.3-meter (70-foot) radius from the center of the original structure due adverse weather conditions.

5.3.5 The furthest recovered fragment of Test 2 was from the north quadrant at 105 meters (341 feet) from the center of the structure and weighed 76 grams. The heaviest recovered fragment was found 37 meters (121.4 feet) from the structure and weighed 8,400 grams.

5.3.6 The calculated inhabited building distance (IBD), or public traffic route distance (PTRD), for this test was 23.3 meters (76.41 feet), and the calculated inter-magazine distance (IMD), or intra-line distance (ILD), was calculated to be 15.798 meters (51.83 feet)[5]. Numerous fragments landed beyond the calculated IBD/PTRD distance.

5.3.7 The fragment map for Test 4 is presented in Figure 28. The origin of the map is the center of the structure. This test produced fragments from all side walls and roof. The farthest fragment measured was 156 meters (512 feet) from the origin and was identified as part of the roof.

5.3.8 The IBD calculated for this test was of 23 meters (75 feet). A vast amount of fragments landed beyond this boundary. The largest fragment collected weighed 11,555 grams, and it landed 31.5 meters (103 feet) from the origin. According to the color of the fragment, it was determined it came off of the roof. This fragment, along with 1,419 of the 3,245 fragments recovered, landed beyond the IBD. The fragment data from these two tests indicate that the slower reacting 7P propellant with the lower surface area produced a larger number fragments beyond the calculated IBD than did the 1P, Test 2.

5.3.9 Originally, it was thought to compare the HD1.3 tests with the HD1.1 tests described in Berglund et al.[31] and Gronsten et al.[32]; however, referring back to the simplified hazard event of Figure 1, it became apparent that there are too many variables to permit a direct comparison. The first and probably most important is that the stimulus of the HD1.1 tests was prompt shock, while that of the HD1.3 tests was combustion. Second, there was no venting of the Kasun structure in the HD1.1 tests. A general observation that can be made between the two sets of tests is relative to the different time regimes that exist between a shock-driven versus a combustion-driven hazard event. There are two orders of magnitude difference in the time response between the pressure versus time of the HD1.1 and Tests 2 and 4 of the HD1.3 tests, shown in Figure 29. The longer, slower pressurization will result in larger fragments, many of a flat, plate-like shape resulting in longer distance projection relative to their mass.

6. Summary/Conclusions

6.1 The thermal stimulus either externally applied (fire) or by internal means is most often seen in a transportation and storage hazard event. The chemical composition, physical state, and geometry of the energetic material coupled with the amount of confinement will define the level of the response that results from the stimulus.

6.2 Basic combustion properties of the HD1.3 item or bulk substance drive the ease of ignition and subsequent combustion behavior of a combustion driven hazard. The ease of ignition by thermal stimulus at low pressure is critical with respect to handling safety. Most of the HD1.3 AP-based propellants readily ignite and burn at ambient pressure, while many HD1.1 nitramine-based explosives are difficult to ignite at relatively low pressures. In contrast, the nitramine-based HD1.1 samples often readily gasify without complete ignition, generating reactive gaseous products that can then contribute to convective burning and DDT. Within a family of energetic materials, the higher the burning rate the shorter the time to complete ignition.

6.3 Burning rate measurements should be extended beyond the range of operational design for understanding hazards response. Low pressure burning rate measurements provide insight into the ease of ignition and potential for extinguishment in a formulation. These data are useful in describing the hazards potential in both handling and storage. The materials that burn well at ambient pressure generally are also the easiest to ignite, making them the most vulnerable in a thermally induced transportation and storage incident. Data from this report would indicate that the HD1.3 substances are the easiest to ignite with the highest burning rate at ambient pressure. High pressure burning rates provide insight into the stability of the burning grain and rate of pressurization. The rate of pressurization relative to the rate of depressurization or venting is critical in the level of reaction violence in a storage situation.

6.4 It can be seen in Equation (3) that as the linear burning rate of the material increases, so too does the mass regression rate. The available surface area of an energetic material, either HD1.1 or 1.3, has an effect on the mass regression rate as well. The higher the available surface area of the energetic, either by manufacture or damage, the higher the mass regression rate of the substance will be. Reaction violence will likely increase as well.

6.5 HD1.3 Tests 2 and 4 were selected from a series of thermally initiated, subscale magazine (Kasun) tests with bulk M1 gun propellant of two geometry types. Both of these tests exhibited choked flow resulting in the failure of the structure. The difference in propellant surface area (small, 1P versus large, 7P grains) was evident in the pressurization and rupture of the structures. The structure containing the higher surface area 1P grain rupture occurred at 1.4 seconds, while the lower surface area 7P grain occurred at 2.3 seconds.

6.6 The structure failed at the roof in both tests and, while not discussed in this report, was due to the construction of the rebar in the concrete rather than by the physical properties of the energetic fill[6]. Plume and subsequent fireball formation were directional with the majority of structural fragment debris originating from the roof of the structure. Structural debris was recovered at distances beyond the IBD calculated for the M1 loading density of these tests. The slower reacting 7P sample appeared to produce more fragments beyond the calculated IBD than the higher surface area 1P sample; however, further testing is needed to validate this observation.

6.7 Addressing the question of unchoked flow (no rupture) or choked flow (rupture with projection of structural debris) is only a partial consideration of the hazards associated with HD1.3 energetic materials. The hazards from the plume exiting the structure for unchoked flow (Figure 21) and the fireball following rupture of the structure for choked flow (Figure 22) need to be addressed. If a person was directly in the plume or fireball even in these relatively small tests, they would have quickly become a fatality due to the high temperatures of the exit plume. Even if a person was not directly in the plume or fireball, the radiation hazard in terms of heat flux and exposure time might still result in fatalities. DODM 6055.09[5] has recently been modified to include prevention of second-degree burns using exposure times less than the time given in Equation (5) :

$$t = 200\, q^{-1.46} \tag{5}$$

where

q = heat flux, kW/m^2

t = exposure time, seconds

6.8 A thermal flux of 10 kW/m^2, for example, will result in second-degree burns at 6.9 seconds exposure time, while a heat flux of 15 kW/m^2 will cause second-degree burns at 3.8 seconds exposure time. A flux of 5 kW/m^2 gives 19.1 seconds before the onset of second-degree burns, giving a modest amount of time to recognize the threat and take evasive action. The petroleum industry uses a criterion of 5 kW/m^2 at the boundary fence as one of their safety criterion for fire in refineries[33]. Fortunately, the heat flux diminishes roughly as $1/d^2$ with d being the distance from the plume or fireball.

6.9 Both Tests 2 and 4 resulted in large directional plumes followed by a fireball upon structural failure. Calculated fireball diameters of 88 feet (27 meters) and 86 feet (26 meters) from DODM 6055.09-M[5] were surpassed in both tests. Temperature and thermal flux measurements indicate a thermal hazard beyond the current regulatory descriptors. These studies are being used to improve the descriptors relative to the HD1.3 class ; however, further testing is warranted.

7. Needs

7.1 The investigations summarized in this document serve to highlight a number of areas where more data and further studies are needed. The hazard division 1.3 is very broad and study is needed for more than a single substance type and/or item. The M1 propellant tested in the subscale tests is not the most energetic of the bulk gun propellants that might be found in a storage or transportation environment. A further complication is that in the United States, mixed storage is common; for example, an all up round (AUR) might be composed of an HD1.1 warhead, an HD1.3 rocket motor, and numerous HD 1.4 auxiliary items. The AUR will be stored at the highest hazard designator, HD1.1, but contain substances at hazard levels that are more sensitive to a thermal stimulus than the HD1.1 explosive fill.

7.2 Ignition and burning rate measurements are commonly performed on solid rocket propellant for performance purposes, but these measurements are rarely performed on explosives and pyrotechnics. The energetic fills used in both HD1.1 and HD1.4 items should be characterized. Measurements at pressures above and below the operating regime of the solid rocket motor are also rare but should be considered for evaluation of the hazard threat. Low pressure burning rates of gun propellants are of particular interest.

7.3 Confinement scenarios that closely simulate those found in transportation and storage need to be investigated. Light confinement of shipping containers as well as the heavy confinement found in an earth covered magazine should be studied. The 2 meter square concrete structure, while large in comparison to the laboratory tests, is relatively small when compared to many storage magazines, and scaling factors are unknown. The loading densities used in the HD1.3 subscale tests was aimed at identification of the differences between choked and unchoked venting and did not address loading densities of the average magazine that are often much higher than the loading densities in the 2 m × 2 m × 2 m structures.

7.4 Packing arrangements and loading density should be studied to gain a better understanding of the flame spreading ability within the confining environment in addition to the contribution of dunnage to the combustion driven event.

References

1) T. L. Boggs, K. P. Ford, and J. Covino, NAWCWD TM 8668, Naval Air Warfare Center Weapons Division (2013).
2) Public Law (Title 10, Chapter 141, Sub-Section 2389),
3) Department of Defense Ammunition and Explosives Hazard Classification Procedures, TB 700-2 (Army), NAVSEAINST 8020.8C (Navy), TO 11A-1-47 (Air Force), DLAR 8220.1 (Defense Logistics Agency).
4) A. I. Atwood, Proc. Department of Defense Explosives Safety Board, Portland, Oregon, July 2010.
5) Office of the Deputy Under Secretary of Defense (Installations and Environment), DODM 6055.09-M, Vol. 1, Enclosures 8 and 9, Washington, D.C. (2008).
6) A. D. Farmer, K. P. Ford, J. Covino, T. L. Boggs, and A. I. Atwood, NAWCWD TM 8742, Naval Air Warfare Center Weapons Division (2015).
7) A. D. Farmer, K. P. Ford, J. Covino, T. L. Boggs, and A. I. Atwood, NAWCWD TM 8764, Naval Air Warfare Center Weapons Division (2017).
8) L. Allain, SNPE, NT No. 153/91/-S/TS/NP, 63 pp (1991).
9) W. R. Herrera, L. M. Vargas, P. M. Bowles, F. T. Dodge, and W. E. Baker, Southwest Research Institute, San Antonio, Texas, (1984). Contract MDA903-82-C-0526, SwRI Project 01-7327, 188 pp.
10) L. H. Caveny and M. Summerfield, Proc. 10th JANNAF Combsution Meeting. CPIA Pub. 243, Vol. III, 133–156 (1973).
11) L. T. DeLuca, L. H. Caveny, T. J. Ohlemuller, and M. Summerfield, AIAA J., 14, 940–948 (1976).
12) A. D. Baer and N. W. Ryan, AIAA J., 3, 884–889 (1964).
13) A. I. Atwood, C. F. Price, and T. L. Boggs, Proc. 22nd International Annual Conference of ICT, 44–1 to 44–15 (1991).
14) A. I. Atwood, Proc. 2nd Meeting of EUCASS, Brussels, Belgium (2006).
15) T. J. Ohlemiller, L. H. Caveny, L. T. DeLuca, and M. Summerfield, Proc 14th Symposium (International) on Combustion, The Combustion Insititute (1972).
16) A. I. Atwood, C. F. Price. P. O. Curran, and N. G. Zwierzchowski, Proc. 25th JANNAF Combustion Meeting, CPIA Publication 498, Vol. I, 69–81 (1988).
17) T. L. Boggs, C. F. Price, A. I. Atwood, D. E. Zurn, and R. L. Derr, Proc. Seventh Symposium (International) on Detonation, Naval Surface Warfare Center MP82–834, 216–224 (1984).
18) C. Merrill, Challenges in Propellants and Combustion 100 Years After Nobel, [ed.] K.K. Kuo. New York : Begell House (1997).
19) G. P. Sutton, "Rocket Propulsion Elements : An Introduction to the Engineering of Rockets" 5th Ed, New York : Wiley (1986).
20) C. F. Price and A. I. Atwood, Proc. 1991 JANNAF Propulsion System Hazards Subcommittee Meeting. CPIA Pub. 562, 415–432 (1991).
21) T. L. Boggs, J. E. Crump, K. J. Kraeutle, and D. E. Zurn, Prog. in Aeronautics and Astronautics, Vol. 63, 20–48 (1978).
22) C. Price and A. Juhasz, BRL Report 2018, Ballistic Research Laboratory, Aberdeen, Maryland (1977).
23) A. I. Atwood, T. L. Boggs, P. O. Curran, T. P. Parr, D. M. Hanson-Parr, C. F. Price, and J. Wiknich, J. Prop. Power, 15 (1999).
24) Military Specification, MILE-E-81111B (1985).
25) D. T. Bui, A. I. Atwood, and P. O. Curran, Proc. 18th JANNAF Propulsion Systems Hazards Subcommittee Meeting, Cocoa Beach, Florida (1999).
26) A. I. Atwood, D. T. Bui, P. O. Curran, and C. F. Price, Proc. 5 th International Symposium on Special Topics in Chemical Propulsion, Stressa, Italy, Begell House (2000).
27) Advisory Group for Aerospace Research and Development, [ed.] T. L. Boggs and R. L. Derr, AGARDograph No. 316, p. 191 (1990).
28) J. G. Routley, "Fire and Explosions at Rocket Fuel Plant Henderson, Nevada (May 4, 1988)," Federal Emergency Management Agency, United States Fire Administration, National Fire Data Center, Report 021 of the Major Fires Investigation Project. http://www.interfire.org/res_file/pdf/Tr-021.pdf (accessed : 31-January-2018). (online).
29) H. P. Richter, L. R. Boyer, K. J. Graham, A. H. Lepie, and N. G. Zwierzchowski, Proc. Ninth Symposium (International) on Detonation, Portland, Oregon (1989).
30) L. H. Christensen and S. Skudal, Norwegian Defence Estates Agency (Forsvarsbygg), Norway. (FoU Rapport nr.

24/2004.)

31) R. Berglund, A. Carlberg, R. Forsen, G. A. Gronsten, and H. Langberg, FOI, Forsvarsbygg, FOI-R-2202-SE, ISSN 1650−1942 (2006).

32) G. A. Gronsten, R. Berglund, A. Carlberg, and R. Forsen, Using Cased Charges-Kasun III." FOI-R-2749-SE, Forsvarsbygg Report 68/2009 (2009).

33) Society of Fire Prevention Engineers, "Engineering Guide : Predicting 1st and 2nd Degree Skin Burns From Thermal Radiation," SFPE, Maryland (2000).